1

Event Selection

The selection of hadronic events has been developed in the V_{cs} analysis of the Ljubljana Group citeberzen. In the procedure we first apply some very loose cuts on some standard kinematic quantities in order to remove the background channels that are easily distinguishable from the WW events; this also somewhat reduces the systematic uncertainty in our event selection because some channels are not well known from the theoretical point of view, but have nevertheless a clear kinematic signature (e.g. $\gamma\gamma$ channel). The applied cuts are listed as follows:

- The charged multiplicity has to be greater than 8.
- The total multiplicity has to be greater than 25.
- There have to be at least 3 reconstructed natural jets (LUCLUS) with $d_{join} = 6.5$.
- S' has to be greater than 130 GeV.
- The fastest neutral track has to have energy below 50 GeV.
- Sphericity has to be greater than 0.1.
- $\log_{10}$ of χ^2 of kinematic fit has to be less than 2.3.
- reconstructed M_W has to be greater than 50 GeV.
- each of the fitted four jets has to have more than two particles.

In this preselection only about 10% of estimated $W^+W^- \rightarrow 4q$ is lost while the background contamination is decreased almost by an order of magnitude.

For the final selection a probabilistic approach has been developed, which makes the event selection more sensitive to the distinction between the signal and kinematically very similar background (e. g. $Z\gamma$ channel) than stringent selection cuts. The procedure is roughly described as follows: For several kinematic quantities the distributions for expected signal and background are plotted separately and then normalized into probabilities. For each event and the given kinematic quantity (i) a probability that an event is coming from either $W^+W^- \to 4q$ channel or any of the background channels is computed:

$$P_i^{sig}(x_i) = \frac{p_i^{sig}(x_i)}{p_i^{sig}(x_i) + p_i^{bkg}(x_i)}, \tag{1.1}$$

$$P_i^{bkg}(x_i) = 1 - P_i^{sig}(x_i), \tag{1.2}$$

where the $p_i^{sig}(x_i)$ and $p_i^{bkg}(x_i)$ denote the probabilities obtained for a kinematic distribution i for valuex_i for the given event.

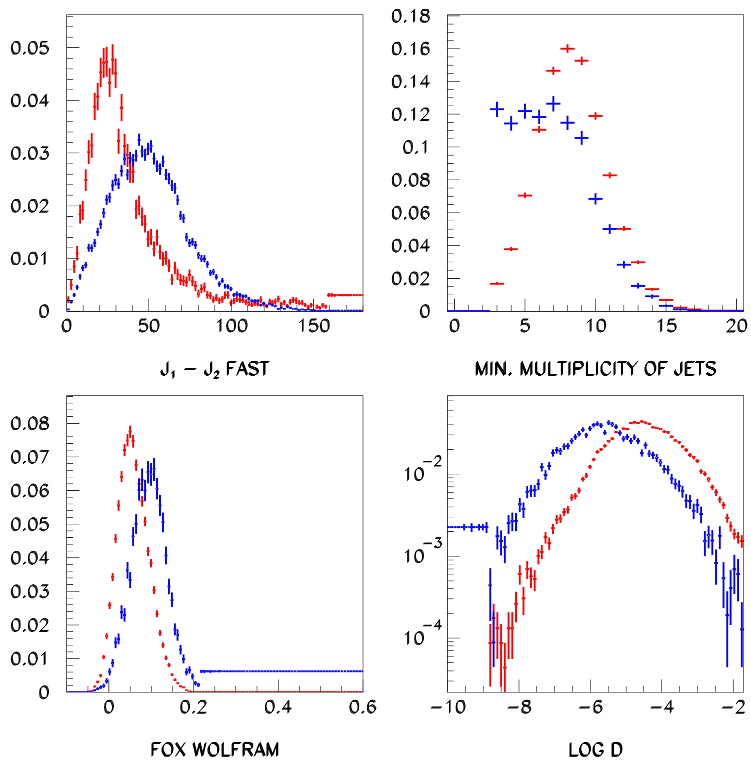

Figure 1.1: An example of probability distributions $p_i^{sig}(x_i)$ (red) and $p_i^{bkg}(x_i)$ (blue) for some of the used kinematic quantities.

Several probabilities for different kinematic quantities are then combined into one (normalized) probability we call the kinematic separator P_{WW}:

$$P_{WW}(\vec{x}) = \frac{\prod_i P_i^{sig}(x_i)}{\prod_i P_i^{sig}(x_i) + \prod_i P_i^{bkg}(x_i)}. \tag{1.3}$$

A final cut which maximizes the product of efficiency and purity is then applied.

1.1 Event selection on '98 D2 data

In the given analysis the following kinematic quantities have been chosen:

- $D_{join}(3 \to 4)$, i.e. the value of D_{join} in Luclus algorithm when four instead of three natural jets are reconstructed.
- Sphericity.
- Angle between the fastest jets.
- Minimal multiplicity in a jet.
- Fox Wolfram momentum.
- Logarithm of the D variable.
- S' as obtained by the SPRIME package.
- Reconstructed M_W.
- Product of the energy ratios of the two jets in both dijets.
- The minimal transverse momentum to the direction of beam axis of 15 most energetic tracks.
- The transverse momentum to the direction of beam axis of a jet pair which is obtained by forcing two jets to be reconstructed.

The selection of used kinematic quantities was based on the motivation to obtain the best possible signal/background separation. It still had to be taken into account that the differences between the Monte Carlo and data distributions should not differ significantly otherwise this would induce a large systematic uncertainty of the selection efficiency. The latter has been checked by using merged Z^0 events as described later on in systematic studies.

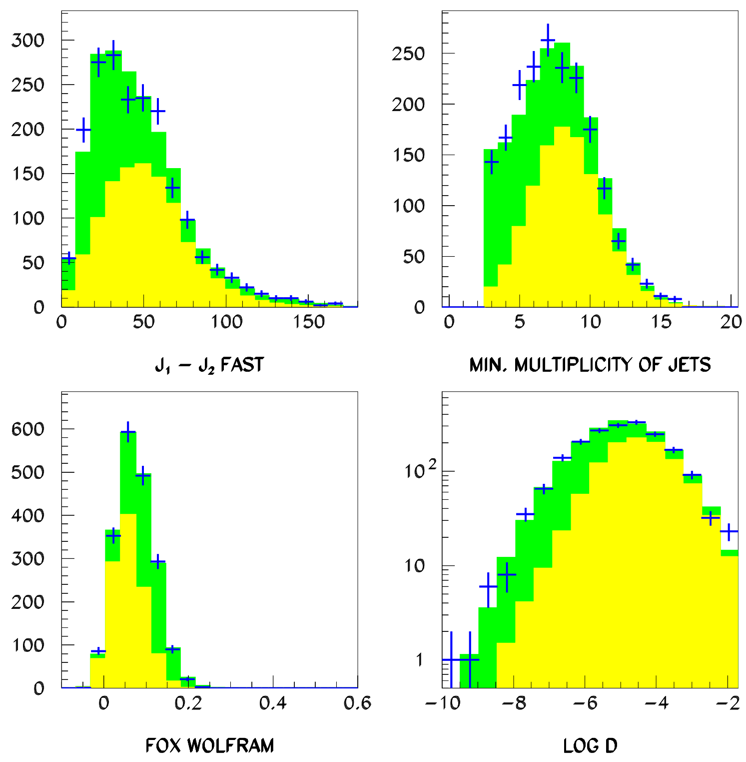

Figure 1.2: An example of kinematic distributions used for P_{WW} construction. The signal MC is denoted in green, background in yellow and data represent the blue error bars.

The following background channels have been taken into account:

- The semileptonic decay channels,
- Single W decays - $We\nu$,
- ZZ decays,
- Single Z decays ,
- The $Z\gamma$ channel,
- Two photon decay channels.

Other background channels (e.g. Bhabha and Compton scattering) have been probed as well but fail to pass the preselection cuts.

In case of 1998 data sample (D2 processing) with luminosity $\mathcal{L} = 157.65 pb^{-1}$ 1331 events survive the cut $P_{WW} = 0.4$. From the simulated sample one obtains the estimated efficiency to be $\epsilon = (86.6 \pm 0.2)\%$ and purity $P = (74.4 \pm 0.4)\%$. The main background contributions come from the $Z\gamma \to qq\gamma$ and $W^+W^- \to qq\tau\nu_\tau$ kinematic channels.

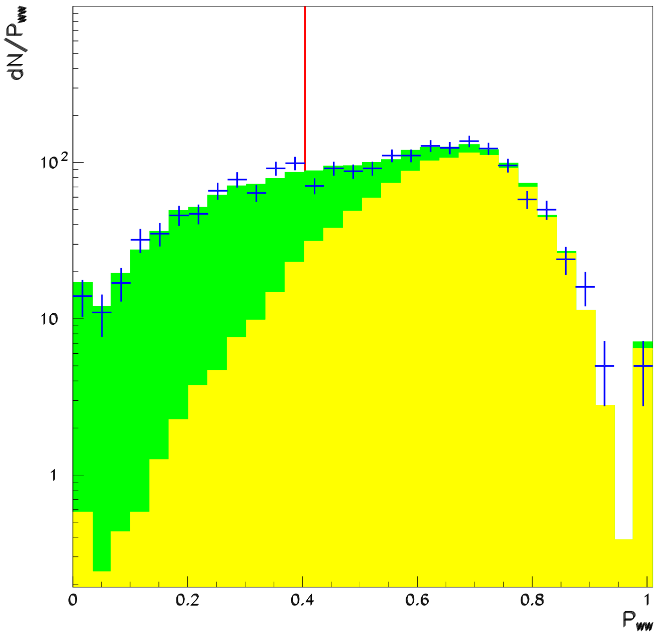

Figure 1.3: TheP_{WW} distribution for '98 data and MC. The signal MC is denoted in green, background in yellow and data represent the blue error bars. The cut is marked as a red line.

2

Event reconstruction

In the event reconstruction of the channel $W^+W^- \rightarrow qqqq$ exactly four jets are forced to be reconstructed using the LUCLUS clustering algorithm. Consequently we are left with three possible combinations of a jet pair originating in a W decay.

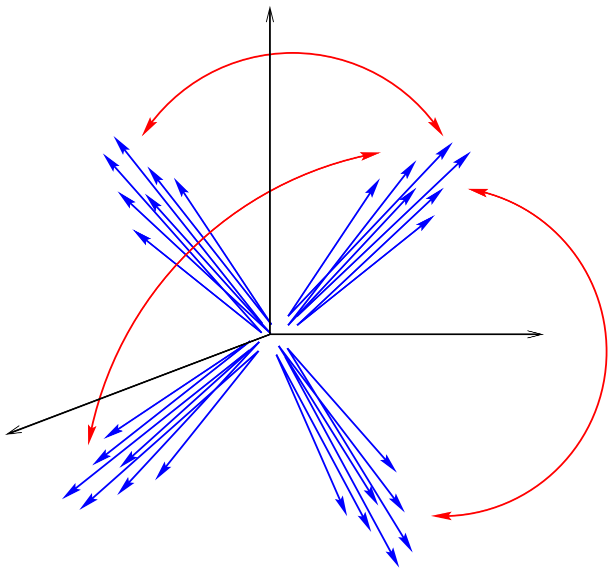

Figure 2.1: The three possible pairing combinations.

To pair the correct jets together a 5C kinematic fit is performed using the PUFITC+ routine requiring the total full momentum to be conserved and the reconstructed masses of the two chosen dijet pairs to be equal. Subsequently the χ^2 of the kinematic fit and the reconstructed M_W for all the three combinations are put into a neural network which chooses the best possible combination.

To determine the pairing efficiency a MC study was performed assigning parent quarks to reconstructed jets basing on the smallest quark – jet angle, which proved to be an efficient enough criterion. With such assignment the neural network has been trained and the estimated pairing efficiency was determined to be $\epsilon_{pair} = 78.6 \pm 0.3\%$.

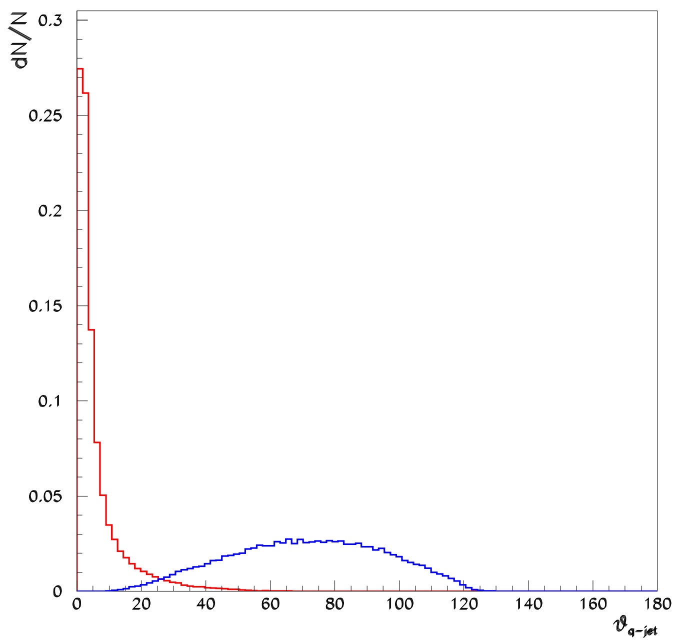

Figure 2.2: The minimal polar angle between the direction of the original quark and reconstructed jet (red histogram). The second smallest angle is drawn for comparison (blue histogram). The smallest quark-jet angle is evidently a good criterion for quark-jet assignment.

Since neither the quark flavor nor the charge of the parent W cannot be determined directly the jet charge was used to tag a dijet pair to originate in a W^- decay:

$$Q_{jet} = \frac{\sum_i q_i \left(\vec{p_i} \cdot \vec{T_{jet}}\right)^{0.7}}{\sum_i \left(\vec{p_i} \cdot \vec{T_{jet}}\right)^{0.7}}. \tag{2.1}$$

In the above expression q_i and $\vec{p_i}$ denote the charge and momentum of a particle belonging to the given jet and $\vec{T_{jet}}$ denotes the reconstructed jet direction.

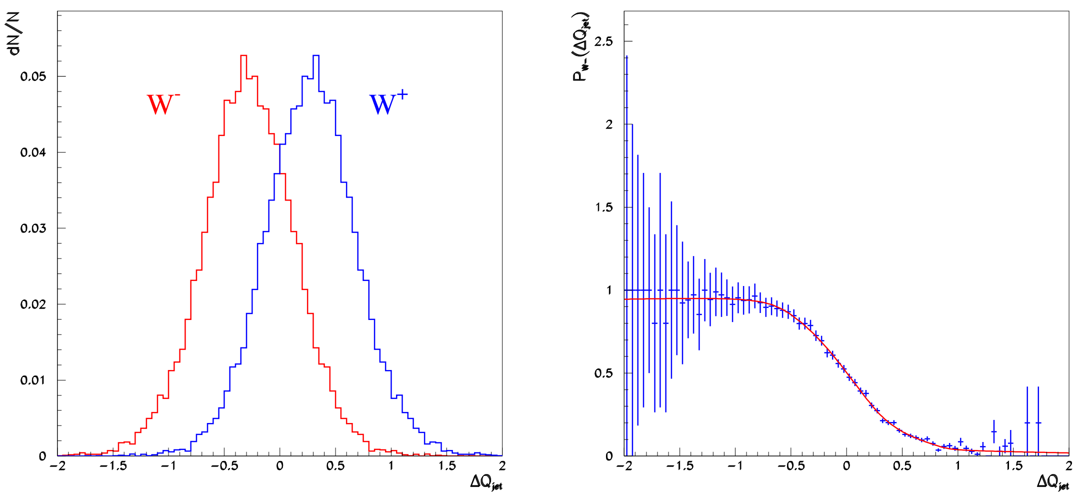

Figure 2.3: The distributions of dijet pairs coming from $W^{\pm}$ with respect to the ΔQ and therefrom constructed $P_{W^-}(\Delta Q)$ on the second histogram

To resolve the ambiguity the jet charge distribution of true W^-(as assumed by the quark jet association mentioned above) was used to construct a probability $P_{W^-}(\Delta Q)$ that a dijet comes from a W^- decay as a function of the difference of both dijet charges $\Delta Q = (Q_{jet}1 + Q_{jet}2) - (Q_{jet}3 + Q_{jet}4)$. By tagging a (correctly associated) dijet pair as coming from a W^- decay when having $\Delta Q < 0$ the computed efficiency from MC studies was determined to be $\epsilon_{\Delta Q} = 75.6 \pm 0.3\%$. Various attempts have been made to improve the charge separation by redefining the jet charge expression and using other quantities as weights (e.g. rapidity) however none of the variations has proved to be significantly better so far.

3

Method of analysis

The principal motivation in our analysis was to determine the separate contributions of angular distribution and measured $W^+W^- \to 4q$ cross section to the accuracy of the determination of TGC parameters. Thereby, the cross-section more accurately measured by the DELPHI W cross-section team could in principle be used. We measured the TGC values according to the so called Baur set, i.e. Δg_Z^1,λ_γ and $\Delta\kappa_\gamma$, performing the measurement for each parameter separately, while assuming the other two to have the Standard Model value.

3.1 Angular distribution analysis

In our measurement of the angular distribution dependence on the TGC parameters the distribution of events as a function of $W-$ production angle was chosen. Because of the charge assignment uncertainty mentioned in the previous chapter a new variable XQ was constructed:

$$XQ = P_{W^-}(\Delta Q)\cos\theta_W \;-\; (1 - P_{W^-}(\Delta Q))\cos\theta_W \tag{3.1}$$

where both possible W^- production angles were included, which in our case amounts to $\pm\cos\theta_W$, each weighted with the appropriate probability of the pair to be coming from W^- decay $P_{W^-}(\Delta Q)$ described in previous chapter. Analysis was also done using the $\cos\theta_W$ selected with the criterion of $\Delta Q < 0$, however this variable turned out to have a somewhat weaker sensitivity – since we put less information into the method –as well as a higher liability to give less probable results because we have a binomial probability of picking events with a certain sign $\pm$ of $\cos\theta$ and this in case of a small statistics can shift the inclination of the distribution towards erratic values of TGC parameters (c.f. systematic studies).

Consequently a binned likelihood fit was performed using the multinomial probability:

$$p_i = \frac{\bar{N}_i^{bkg}}{N} + \frac{N - \bar{N}^{bkg}}{N} \frac{\bar{N}_i^{sig}(\alpha)}{\bar{N}^{sig}(\alpha)}, \tag{3.2}$$

where p_i is the multinomial probability in bin i, $\bar{N}_i^{bkg}$ and $\bar{N}_i^{sig}$ are the expected number of signal and background events scaled to the measured luminosity in i-th bin, N is the total number of measured events and $\bar{N}^{bkg}$ and $\bar{N}^{sig}$ are total numbers of expected background and signal respectively. The $\bar{N}_i^{sig}(\alpha)$ and consequently $\bar{N}^{sig}(\alpha)$ are functions of TGC parameters denoted by α, whereas the background is assumed to be independent of TGC-s. As one can see the expected signal probability is scaled to the number of $N - \bar{N}^{bkg}$ in order to get rid of the measured cross-section dependence on TGC-s.

A binned log likelihood is performed at 41 discrete values of the given TGC parameters, i.e. in range $[-2, 2]$ in steps of 0.1 of a selected parameter, while the other two were kept at the Standard model value. The $ln\mathcal{L}$ expression is therefore:

$$ln\mathcal{L}(\alpha_j) = \sum_i n_i \; \ln \left(\bar{N}_i^{bkg} + \frac{N - \bar{N}^{bkg}}{\bar{N}^{sig}(\alpha_j)} \bar{N}_i^{sig}(\alpha_j) \right) \tag{3.3}$$

where n_i is the number of measured events in the i-th bin and $\bar{N}_i^{sig}(\alpha_j)$ denotes the expected number of $WW \to 4q$ events in i-th bin at a discrete α_j value $j = 1...41$.

3.2 Re-weighting procedure

Different angular distributions for the discrete TGC values were obtained by re-weighting the Standard model Fullsim Pythia sample using the EXCALIBUR generator based re-weighting routine by F. Cossutti, where each event was re-weighted with a fraction of the squared matrix elements computed by EXCALIBUR:

$$wt_i = \frac{|M(\vec{\Omega}_i, \alpha_j)|^2}{|M(\vec{\Omega}_i, \alpha = SM)|^2} \tag{3.4}$$

where $\vec{\Omega}_i$ is the full kinematic information consisting of the generated parameters for a given event, $|M(\vec{\Omega}_i, \alpha_j)|^2$ is the value of the matrix element squared for the event i at a α_j value and SM denotes the standard model value.

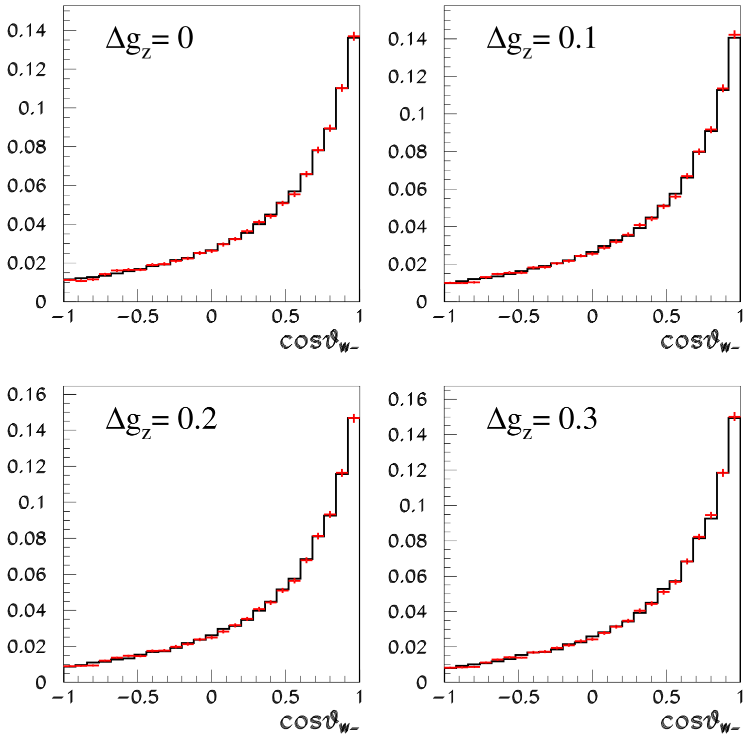

Figure 3.1: The agreement between generated excalibur distribution with respect to the cosine of W^- production angle (histogram) and re-weighted Pythia MC (red error bars) for a few values of Δg_Z^1.

3.3 Total cross-section analysis

The re-weighted distributions were scaled to the TGC-dependent cross-section $\sigma_{WW\to 4q}(\alpha_j)$ which was computed using the EXCALIBUR generator and has as predicted a parabolic dependence on TGC-s. The expected number of $ww \to 4q$ events at a given luminosity $\mathcal{L}$ is therefore :

$$\bar{N}^{sig}(\alpha_j) = \mathcal{L}\ \sigma_{WW\to 4q}(\alpha_j)\ \frac{\sum_i^{sel} wt_i(\alpha)}{\sum_i^{gen} wt_i(\alpha)} = \mathcal{L}\ \sigma_{WW\to 4q}(\alpha_j)\ \epsilon(\alpha_j) \tag{3.5}$$

where in the numerator we sum over the weights of all selected and in denominator of all generated events. Consequently $\epsilon(\alpha_j)$ is the selection efficiency as a function of TGC parameters.

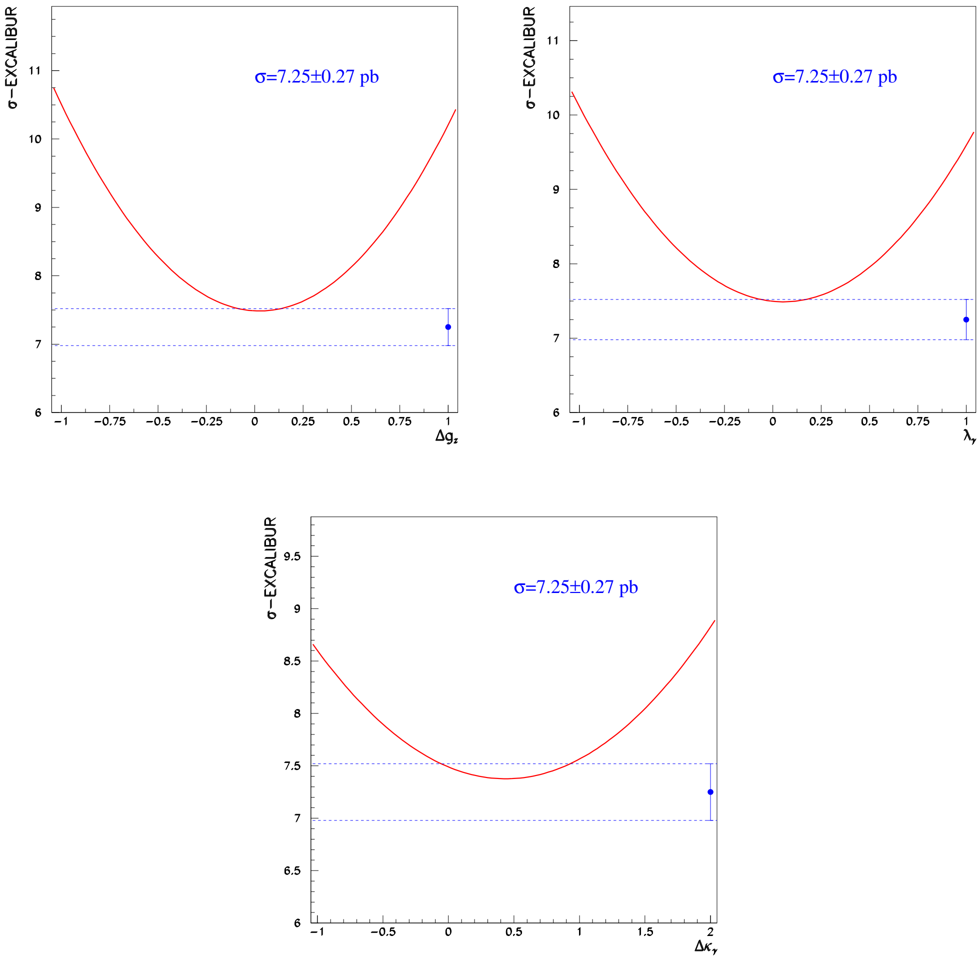

Figure 3.2: The cross-section dependence on TGC parameters (red curve) is evidently parabolic. The value of the cross-section measured in our analysis to be $\sigma(W^+W^- \to 4j) = 7.25 \pm 0.27pb$ is also plotted (blue error bar).

In determination of TGC's from the $\sigma(W^+W^- \to 4j)$ a binned Poisson $ln\mathcal{L}$ fit to the total number of observed events is performed, using the expected number of simulated events as a function of TGC parameters.

$$ln\mathcal{L}(\alpha_j) = Nln(\bar{N}^{bkg} + \bar{N}^{sig}(\alpha_j)) - (\bar{N}^{bkg} + \bar{N}^{sig}(\alpha_j)). \tag{3.6}$$

To obtain the final the combined $ln\mathcal{L}$ consisting of both contributions (i.e. angular and total cross-section dependence) we sum both $ln\mathcal{L}$ expressions and get an expression which is basically extended maximum likelihood.In all the three cases we finally minimize the $-ln\mathcal{L}$ expression to get the measured values of the TGC parameters.

4

Results for '98 D2 data

As already mentioned we have used the distribution of the data and MC over the so called XQ variable to obtain the values of the trilinear gauge coupling parameters from the presupposed distribution dependence. A data – Monte Carlo comparison with MC signal re-weighted to $\Delta g_Z^1 = -0.1$, which is the closest re-weighted value to the one measured, is plotted below.

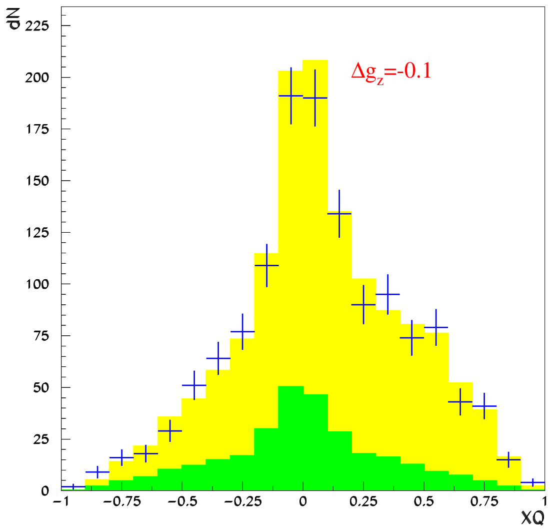

Figure 4.1: Data - MC comparison with MC signal re-weighted to $\Delta g_Z^1 = -0.1$. Expected signal distribution is plotted in green, exp. background distribution in yellow and data are plotted as blue error bars.

For the separate analysis of angular distribution dependence on TGC-s using the multinomial log likelihood we obtained the following results which are represented on histograms below:

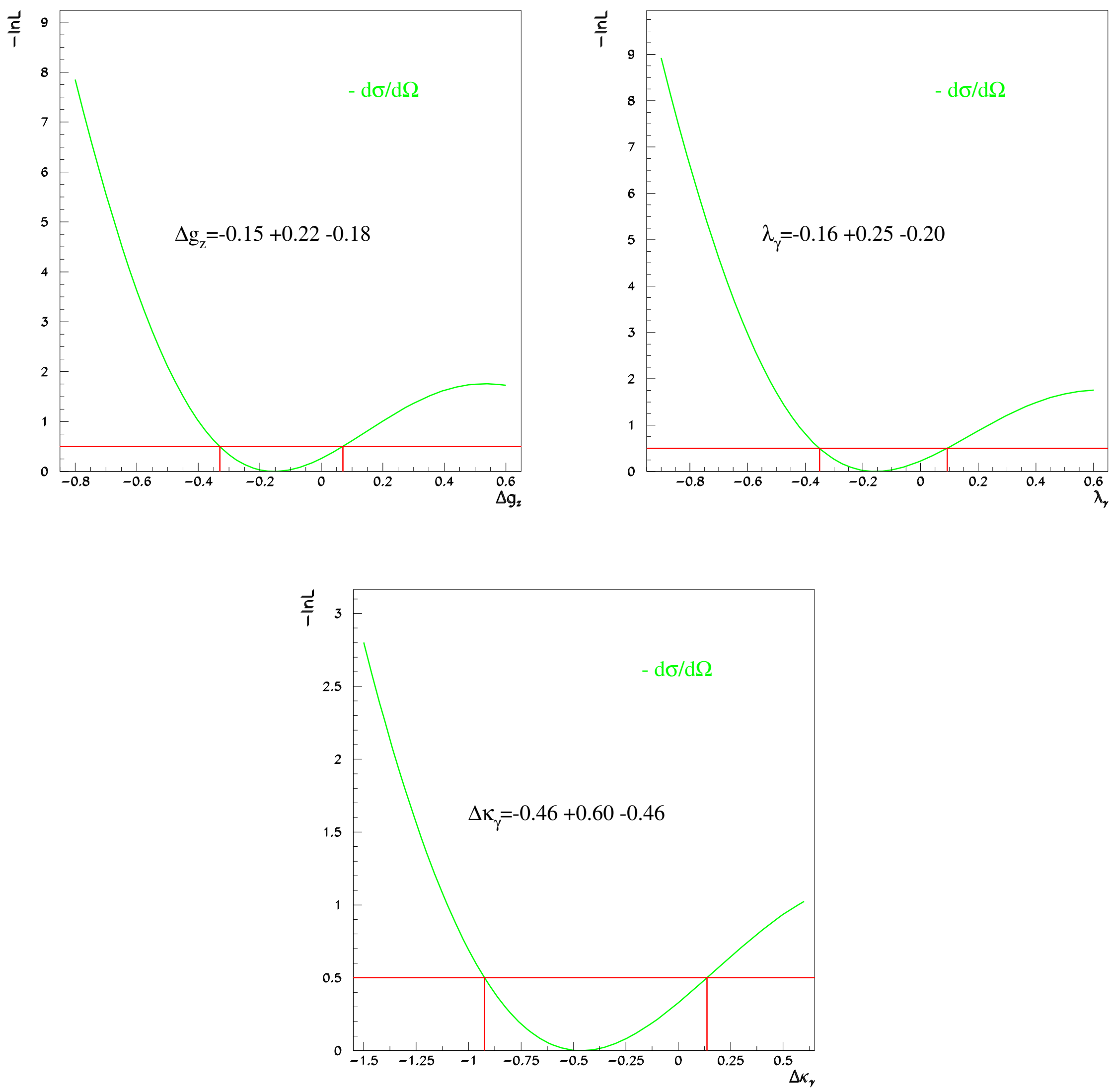

Figure 4.2: The multinomial log likelihood curves for the three measured TGC parameters. The red line marks the errors obtained from the curve (0.5 above the min. value according to conventions). It is evident that the likelihood curves are strongly asymmetric in the positive region. The observed reasons for this will be described in the systematics section.

In the analysis of total cross-section dependence on TGC-s using the Poisson log likelihood we obtained the following results which are represented on histograms below:

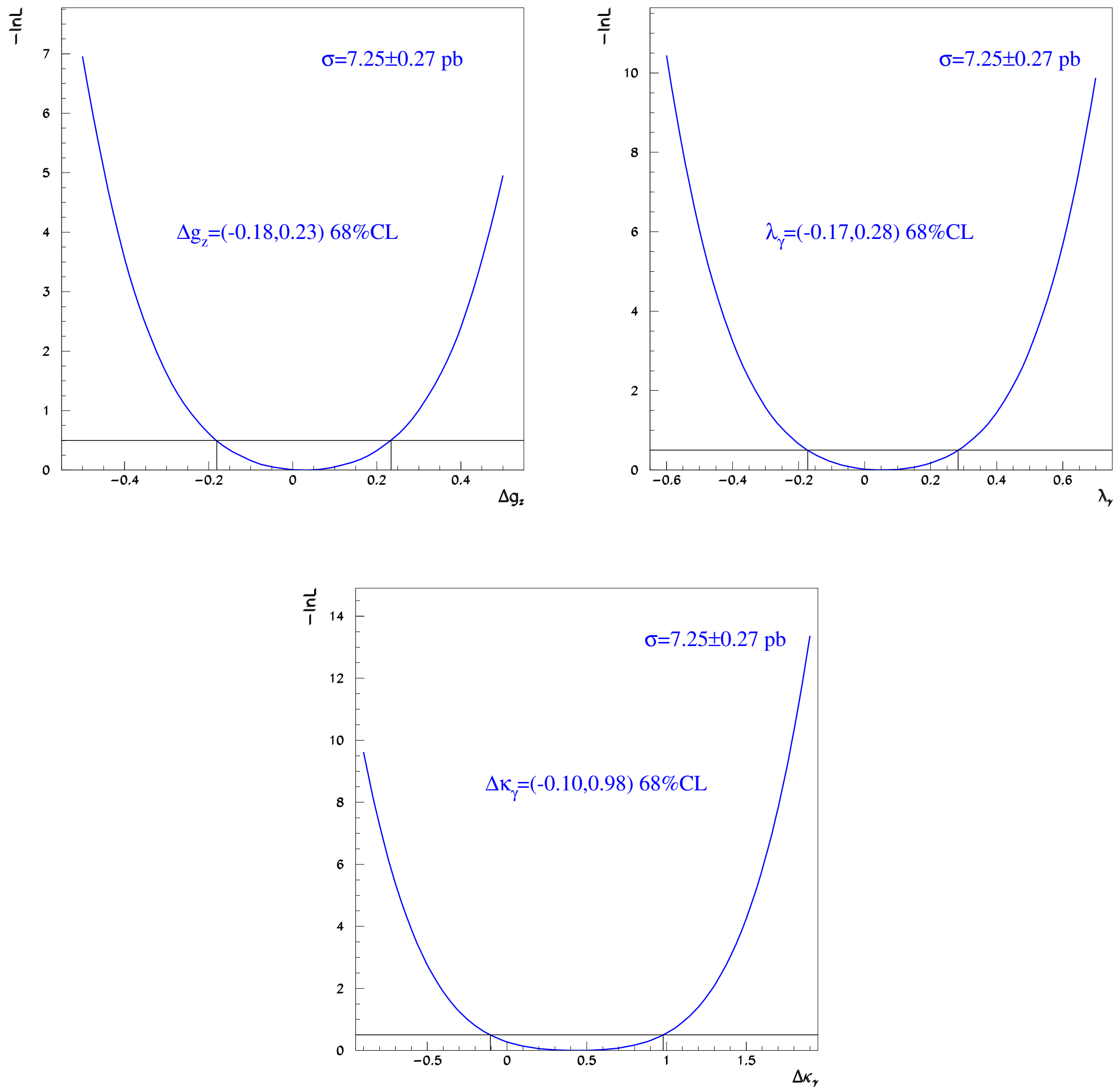

Figure 4.3: The Poisson log likelihood curves for the three measured TGC parameters. The red line marks the errors obtained from the curve (0.5 above the min value according to conventions). The curves are evidently symmetric, but since in general a degenerate curve with two minima can be obtained only the 68% confidence intervals are quoted. In case of our analysis only one minimum was obtained because the measured cross-section lies below the minimum of the theoretical dependence of total $\sigma(W^+W^- \rightarrow 4q)$ (c.f. fig 3.2). Therefore we have a one minimum solution which is not the general case.

Eventually the results from both measurements were combined by adding the likelihood curves obtained from angular distribution and total cross-section measurement; subsequently the combined values were again obtained by minimization of $-\ln\mathcal{L}$.

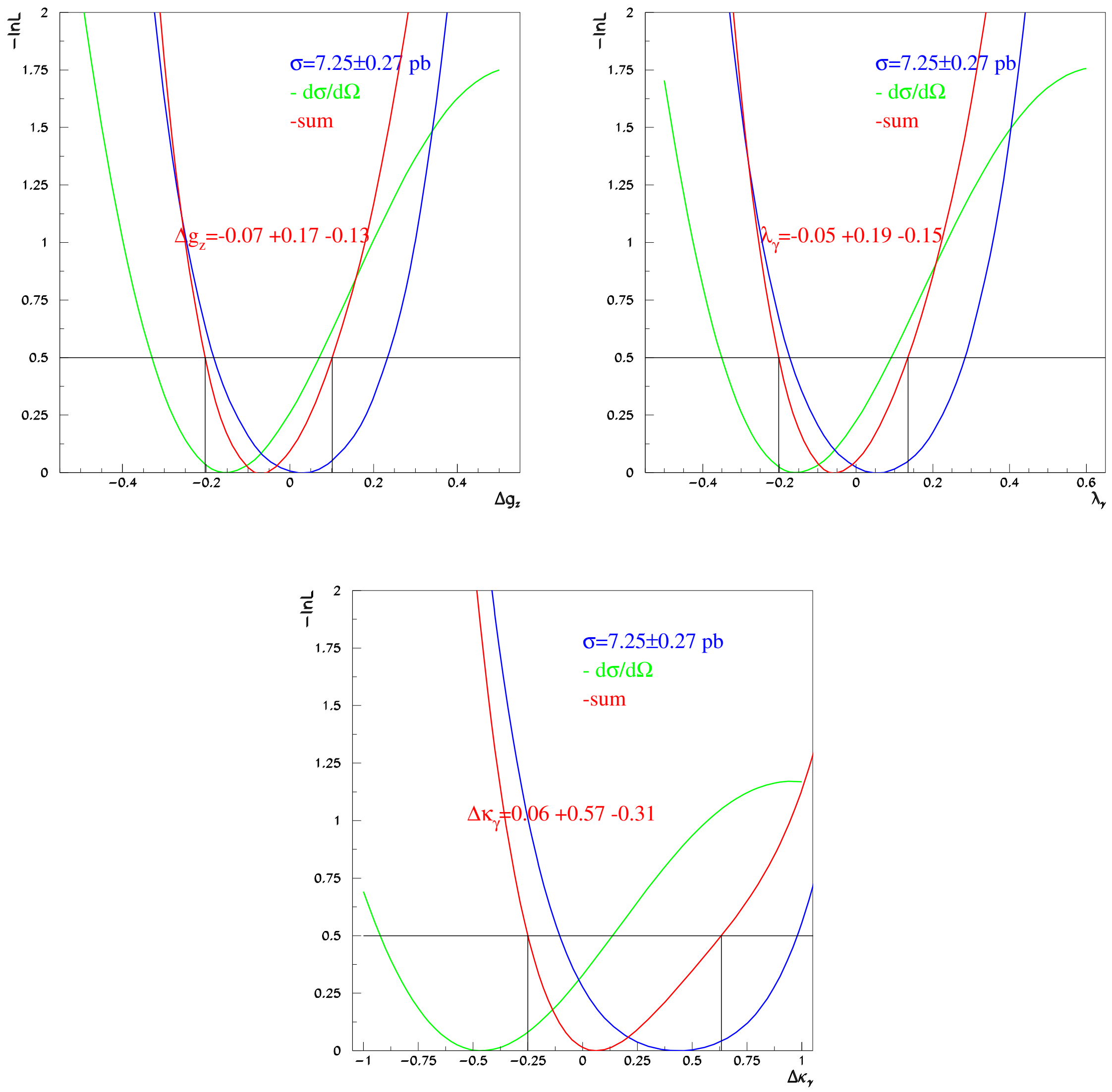

Figure 4.4: The multinomial log likelihood curve (green), Poisson log likelihood curve (blue) and their sum (red) are drawn. The black lines denote the errors obtained in the measurement.

In conclusion the results obtained with the 1998 data sample D2 for the Baur set of TGC parameters are listed in the following table with statistical errors quoted.

method	Δg_z	λ_γ	$\Delta\kappa_\gamma$
Ang. distrib.	$-0.15^{+0.22}_{-0.18}$	$-0.16^{+0.25}_{-0.20}$	$-0.46^{+0.60}_{-0.46}$
$\sigma(W^+W^- \to 4j)$	[-0.18,0.23]	[-0.17,0.28]	[-0.10,0.98]
Combined	$-0.07^{+0.17}_{-0.13}$	$-0.05^{+0.19}_{-0.15}$	$0.06^{+0.57}_{-0.31}$

Table 4.1: Results for the 1998 data sample D2 with quoted statistical errors

None of the three results (i.e. angular distribution, total cross-section and combination) exclude the Standard Model prediction of $\Delta g_z = 0$, $\lambda_\gamma = 0$ and $\Delta\kappa_\gamma = 0$. The measured cross-section contribution evidently improves above all the accuracy in the positive range of our measurements.

5

MC Studies & Tests

A series of 'fast' MC experiments was performed by taking a SM Fullsim sample, varying the contents of each bin in the XQ distribution of events within the statistical error and each time performing a $ln\mathcal{L}$ fit. Thereby 10000 MC experiments were made, which enabled the determination of expected errors and biases. Because of a limited number of available MC events it was decided against the 'bootstrap' technique, i.e. dividing a large MC sample into several small samples by random choice of events with numbers corresponding to the luminosity on data, since that would enable us to do only a small number of MC experiments. The 'fast' MC experiments approach on the other hand offers a practically unlimited statistics, even though its results might give more conservative estimates.

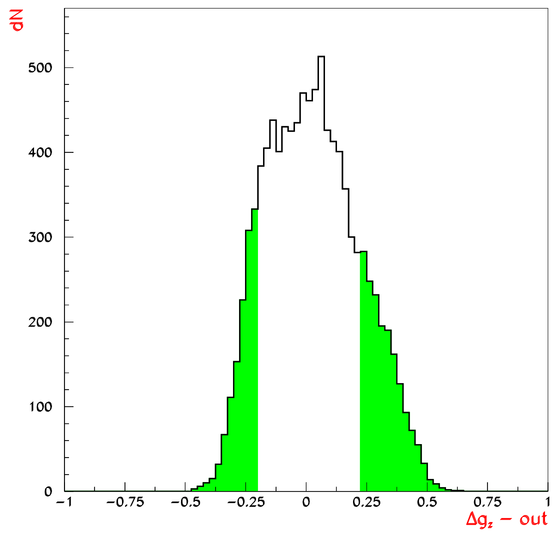

Figure 5.1: The distribution of obtained Δg_Z^1 values while repeating fast MC experiments taking the SM distribution as the initial value. The region excluded from the 86% CI is drawn in green.

Comparison of the obtained results on 189 GeV D2 data with expected errors is shown on the following pictures. The expected errors were defined as the interval which excludes $(1-\epsilon)/2$), in our case $\epsilon = 0.68$ (86% CI), of measurements on each side of the distribution of the TGC parameters obtained through these fast MC experiments (figure 5.1). The expected errors obtained by using the *optimal observables* as the distribution parameter are also drawn for comparison.

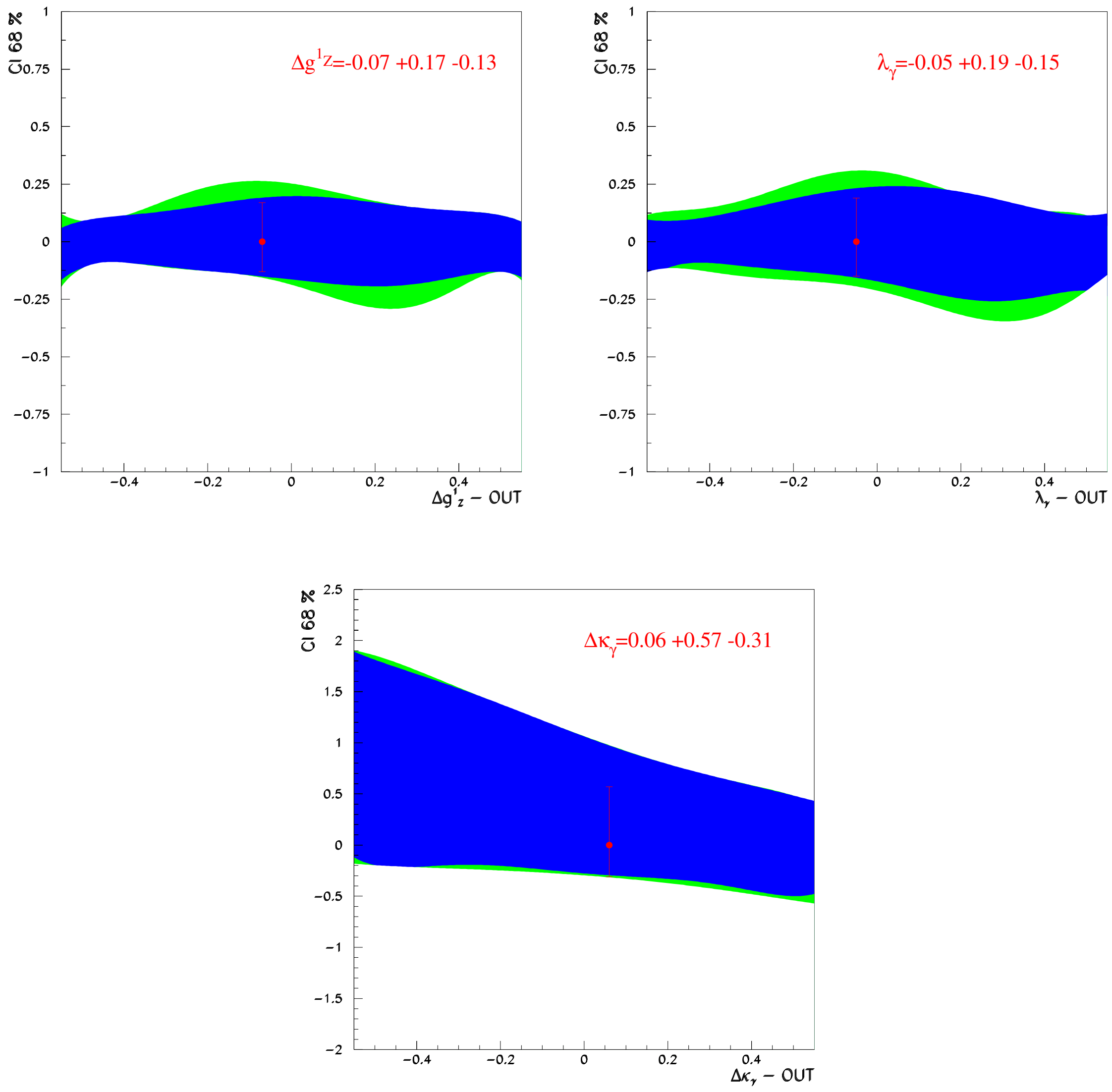

Figure 5.2: Distribution of expected errors according to TGC parameters. The green area is the exp. error obtained from folded $\cos\theta_{W^-}$ and the blue area is the expected error obtained from folded optimal observables for comparison. The obtained result is drawn as a red error bar.

From these distributions the probability to obtain a measured result with the stat. errors less or equal to the measured ones was calculated as listed below:

- In case of Δg_Z^1: $P = 24.8 \pm 0.4\%$.
- In case of λ_γ: $P = 29.8 \pm 0.4\%$.
- In case of $\Delta\kappa_\gamma$: $P = 39.9 \pm 0.5\%$.

Inquiries were made concerning the shape of the multinomial likelihood curve. For this scope 10^5 MC events were generated at different values of TGC-s in order to analyze the dependence of the angular distribution on TGC parameters. From these studies it has been determined that the angular distributions indeed do not change uniformly with variation of TGC-s but decrease in sensitivity in the range of positive values. It is also evident that the most sensitive to changes in the angular distribution is the Δg_Z^1 followed by λ_γ and $\Delta\kappa_\gamma$ which is considerably less sensitive than the other two variables.

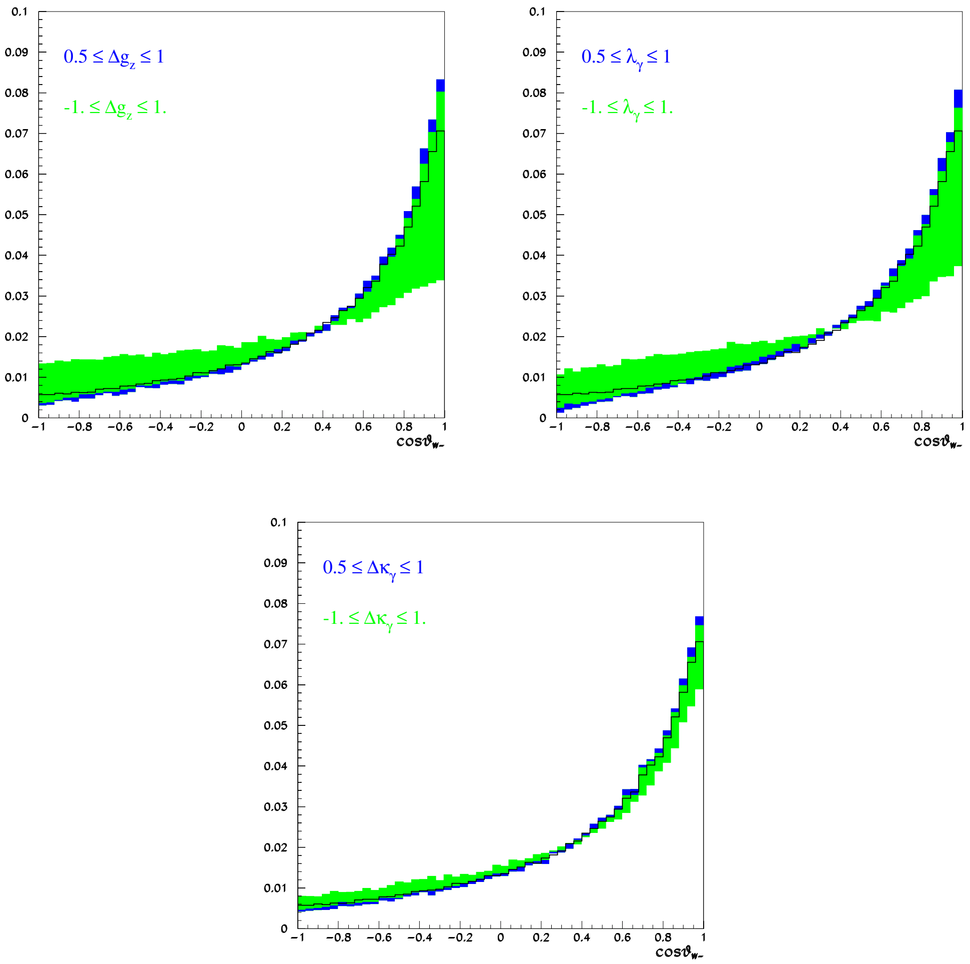

Figure 5.3: Dependence of distribution shape on TGC-s. The green are is the change of slope in interval [-1,1] and in blue the evidently small change in interval [0.5:1] in case of Δg_Z^1. Black histo is the SM distribution.

In a series of Monte-Carlo experiments the accuracy of our method was estimated. First a Standard Model MC sample was taken and a multinomial $ln\mathcal{L}$ was performed to determine the loss of accuracy due to incorrect pairing and wrong W^- charge assignment. The results are given in the following table in percent loss:

TGC par.	Correct pairing	reconstructed
Δg_z	44 %	64 %
λ_γ	47 %	65 %
$\Delta\kappa_\gamma$	43 %	86 %

Table 5.1: The table gives the percent for which the measured errors are greater than the ideal case of correct pairing and charge estimation. The values obtained for $\Delta\kappa_\gamma$ might seem strange but it has to be considered that this is the least sensitive variable with respect to angular distribution so the errors are very large to start with.

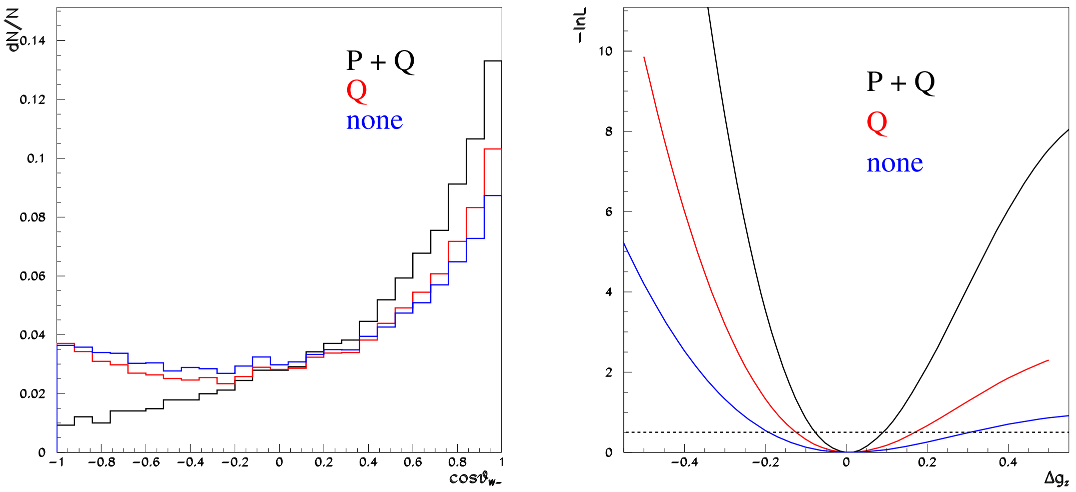

Figure 5.4: Dependence of distribution shape on pairing and charge assignment. The case of correct pairing and charge estimation is drawn in black, the case of correct pairing with charge assignment to dijet pairs according to $\Delta Q < 0$ is drawn in red and the distribution with pairing obtained by the pairing algorithm and charge assignment according to $\Delta Q < 0$ (realistic case) is drawn in red. On the right graph the decrease in sensitivity of the log likelihood curves is drawn for corresponding cases.

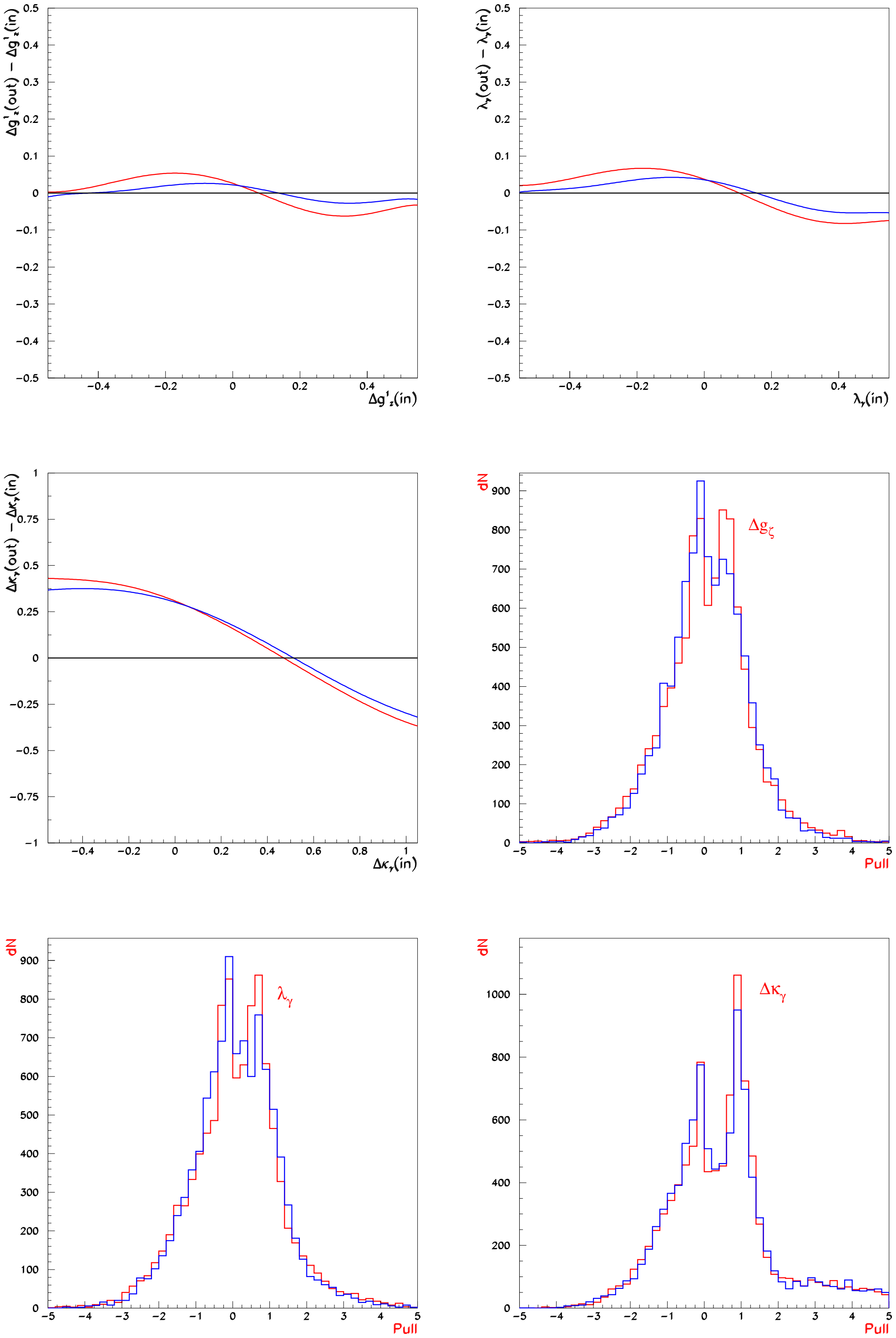

Figure 5.5: Distribution of means and pulls obtained from the fast MC experiments for the three TGC parameters in case of combined log likelihood. The red lines and histos represent the case when XQ variable is used as the distribution parameter and the blue lines and histos are obtained from folded optimal observables for comparison.

From the graphs representing the bias as well as from the pull distributions it is is evident that there is a bias involved in our method. A further inquiry shows that the bias comes solely from the total cross-section contribution to the likelihood, because when the measured value falls below the minimum of the parabola which describes the $\sigma(W^+W^- \to 4j)$ on TGC-s the measured value is discrete and gives simply the parabola minimum value. The double peaked shape of pulls comes from the fact that in case there are two minima in total cross-section measurement and the shape contribution can select either one of them as a global minimum -we are dealing with a strongly asymmetric case.

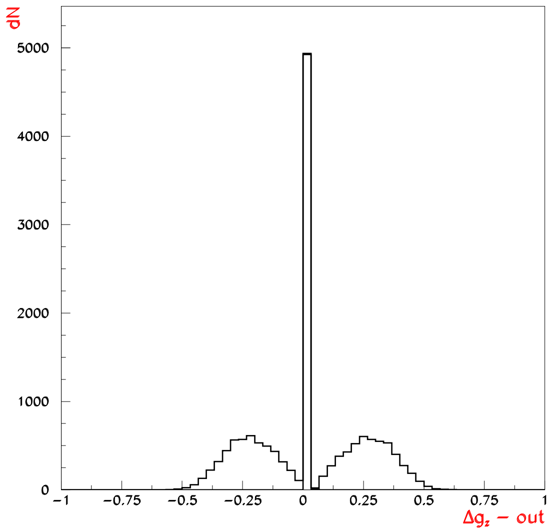

Figure 5.6: Distribution of $\ln \mathcal{L}$ minima obtained in case of total cross-section measurement.

TGC par.	Gen. value	Output - Ang. dist.	Output - Comb.
Δg_z	-0.5	$-0.46^{+0.14}_{-0.14}$	$-0.49^{+0.07}_{-0.06}$
Δg_z	+0.5	$+0.53^{+0.49}_{-0.35}$	$+0.46^{+0.09}_{-0.11}$
λ_γ	+0.5	$-0.63^{+0.16}_{-0.10}$	$-0.53^{+0.08}_{-0.07}$
λ_γ	-0.5	$+0.13^{+1.16}_{-0.24}$	$+0.50^{+0.10}_{-0.12}$
$\Delta\kappa_\gamma$	-1.0	$-1.18^{+0.41}_{-0.40}$	$-0.99^{+0.12}_{-0.14}$
$\Delta\kappa_\gamma$	+1.0	$+0.63^{+1.34}_{-0.75}$	$+1.20^{+0.20}_{-0.28}$

The analysis was done using Pythia generated Fullsim W^+W^- MC. As an additional check the Excalibur generated Fullsim W^+W^- MC was taken instead and the whole analysis was repeated. The results so obtained on data agree with the ones obtained on Pythia within the error on MC statistics.

6

Systematic uncertainties

Several sources of possible systematic errors were studied for each of the TGC parameters separately. Their effect on the measured values (combining angular information and cross-section) is shown in Table 2. Estimation of systematic uncertainties due to individual sources is shortly described below:

- To determine the effect of M_W uncertainty, SM MC sample was re-weighted using matrix elements calculated at masses $M_W = 80.35 \pm 0.10$ GeV. The fit was repeated using these MC samples.

- Number of expected signal and background events was varied according to the integrated luminosity uncertainty of $\pm 1\%$. The fit was repeated.

- Differences between data and simulated samples were estimated by comparing merged Z^0 events. Efficiency of selection procedure was calculated on merged real and simulated Z^0 hadronic events. The relative difference of $\pm 4\%$ was taken into account in the composition of simulated W^+W^- samples used for the fit.

- Possible data/MC discrepancy in $P_{W^-}(\Delta Q)$ distribution was checked by comparing the ΔQ distribution of dijets for which the reconstructed $W^\pm$ direction points in the forward region ($\cos\theta > 0$). By that we obtained sample enriched in W^- decays. Mean value of ΔQ was found to be shifted by ± 0.01 when comparing data and MC sample. Hence the calculation of $P_{W^-}(\Delta Q)$ was repeated by shifting the ΔQ distribution and the fit was redone.

- Expected cross-sections for the signal and background were varied by 2% and 5% respectively.

- Effect of the finite MC statistics was evaluated by random variation of the bin contents in angular distribution within one standard deviation. For each variation the fit to the data distribution was redone.

Source	Δg_Z	λ_γ	$\Delta\kappa_\gamma$
M_W	0.01	0.01	0.02
$\int Ldt$	0.02	0.02	0.08
ϵ	0.05	0.05	0.24
$P_{W^-}(\Delta Q)$	0.01	0.02	0.05
σ_{bkg}	0.03	0.03	0.06
σ_{sig}	0.04	0.04	0.07
MC stat.	0.05	0.05	0.09
Comb.	± 0.09	± 0.09	± 0.29

Table 2. Contributions to systematic uncertainties on TGC parameters due to various sources.